Building layered structures from hydrogen bonded molecular units and 1D metal phosphonate chains: synthesis, characterization and crystal structures of *N,N′*-dimethyl-*N,N′*-ethylenediamine-bis(methylenephosphonic acid), its Ni(II) and Pb(II) complexes

Jiang-Gao Mao, Zhike Wang and Abraham Clearfield *

Texas A&M University, Department of Chemistry, P.O. Box 30012, College Station, TX 77843-3012, USA

The diphosphonic acid, *N,N′*-dimethyl-*N,N′*-ethylenediamine-bis(methylenephosphonic acid) (H$_4$L) **1**, along with its Ni(II) and Pb(II) complexes, have been synthesized and structurally determined. The structure of the diphosphonic acid features a 2D layer built from the molecular units interconnected by hydrogen bonds between phosphonate oxygen atoms and/or nitrogen atoms. Upon complexing with the Ni(II) ion, the diphosphonic acid acts as a tetradentate chelating ligand (2N, 2O), forming Ni(H$_2$L)(H$_2$O)$_2$ **2** molecular units, such units are also interconnected into a hydrogen bonded double layer *via* hydrogen bonds between uncoordinated phosphonate oxygen atoms. The ligand in Pb(H$_2$L) **3** also chelates with a Pb(II) ion tetradentately, however, neighboring Pb(H$_2$L) units are interconnected into a one-dimensional chain along the *c*-axis by a pair of μ^2-chelating and bridging phosphonate oxygen atoms. Such chains are further interconnected into a 3D network *via* hydrogen bonds between uncoordinated phosphonate oxygen atoms. These structures demonstrate the important role of hydrogen bonds in the chemistry of divalent metal phosphonates.

Introduction

Metal phosphonate chemistry has been an area of interest to both inorganic and materials chemists in recent years due to potential applications in the areas of catalysis, ion exchange, proton conductivity, intercalation chemistry, photochemistry, and materials chemistry.[1] Most of the compounds studied are layered species in which the metal octahedra are bridged by phosphonate tetrahedra to form two-dimensional layers that are separated by the hydrophobic regions of the organic moieties.[1] Studies from our group and from others have shown that a variety of metal ions, including group 4 and 14 elements and divalent and trivalent ions, form this type of layered compound.[1–3] Research on metal complexes with phosphonic acids attached with aza-crown ethers and diaza-crown ether show these compounds have many unusual structural features.[1,4] Phosphonic acids with functional carboxylate groups, such as *N*-(phosphonomethyl)iminodiacetic acid (H$_4$PMIDA) are also interesting, since they can adopt various kinds of coordination modes under different reaction conditions.[5–8] Many divalent metal complexes of di- and triphosphonic acids containing an amine group, such as MeN(CH$_2$PO$_3$H$_2$)$_2$ (H$_4$L′) and N(CH$_2$PO$_3$H$_2$)$_3$ have also been synthesized and structurally determined by our group.[9–10] Various types of structures can be formed depending on the degree of the extent of deprotonation on the phosphonate groups, for example, metal phosphonates with 1D double chain (Zn(H$_2$L′)(H$_2$O)), 2D layer (Mn(H$_3$L′)$_2$·2H$_2$O) and 3D network (Zn$_3$(HL′)$_2$) structures have been reported recently in our laboratory.[9] Structures of metal complexes with polyaza-polyphosphonic acids such as derivatives from triazacycles, tetraazacycles and hexaazacycles, usually feature a chelating molecular unit.[11] In these complexes, the nitrogen atoms are coordinated to the metal(II) ion (usually Cu(II) and Co(II)) due to the "macrocyclic effect" and the affinity of the nitrogen atom for the copper(II) or cobalt(II) ion. These chelate ML units are further interlinked into a one dimensional chain by hydrogen bonds between uncoordinated phosphonate oxygen atoms.[12] Very limited structural studies have been carried out on metal phosphonates with diphosphonic acids derived from ethylenediamine,[13] and the structures of their metal complexes are reported to have a chelating molecular unit. We deem that other structural types such as 1D chains and 2D layers should also exist. To expand our studies in this respect, a new diphosphonic acid, *N,N′*-dimethyl-*N,N′*-ethylenediamine-bis(methylenephosphonic acid) (H$_4$L) **1**, along with its Ni(II) and Pb(II) complexes, formulated as Ni(H$_2$L)(H$_2$O)$_2$ **2** and Pb(H$_2$L) **3**, have been synthesized and structurally determined; the Ni(II) complex is a normal chelating molecular compound, whereas the Pb(II) complex features a 1D chain structure. The molecular units of **1** and **2**, as well as the 1D metal phosphonate chain of **3**, are further interconnected *via* hydrogen bonds into a 2D layer. Herein we report their synthesis, characterization and crystal structures.
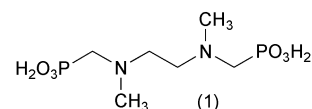
Experimental

Materials and methods

Deionized water used in all experiments was purified to a resistivity of 17.6 MΩ cm with a Barnstead Nanopure II System. All other chemicals were of reagent grade quality obtained from commercial sources and used without further purification. Solution NMR was recorded on a Varian Unity Plus 300 spectrometer. The ^{31}P solid state MAS NMR spectra were obtained on a modified Bruker MSL-300 unit operating at 121.5 MHz, spinning the 7.5 mm zirconium rotors at 2–5 kHz in the NMR probe and using a single pulse sequence (pulse delay = 20 s, 80 transients). H$_3$PO$_4$ (EM Science, 85%, 0 ppm) was used as an

external standard for both solution and solid state ³¹P NMR measurements. Elemental analysis data were obtained from Desert Analytics, Tucson, AZ. Thermogravimetric analysis was carried out with a TA 4000 unit, at a heating rate of 10 °C min⁻¹ under an oxygen atmosphere.

Synthesis of *N,N*'-dimethyl-*N,N*'-ethylenediamine-bis(methylenephosphonic acid) (H₄L) 1. The diphosphonic acid was prepared by a Mannich type reaction according to the procedures previously described.[9] *N, N*'-dimethylethylenediamine (Aldrich, 50 mmol) was mixed with conc. hydrochloric acid (EM Science, 17.0 cm³), deionized water (17.0 cm³) and phosphorous acid (Aldrich, 200 mmol). The mixture was allowed to reflux at 120 °C for 1 hr, then paraformaldehyde (Aldrich, 150 mmol) was added in small portions over a period of 1 hr, and the mixture was then refluxed for one additional hour. After removal of solvents, the gel-like solid was dissolved in 10 ml of deionized water, purified by an ion-exchange procedure yielding 10.7 g (77.5%) of white powder of *N,N*'-dimethyl-*N,N*'-ethylenediamine-bis(methylenephosphonic acid). Its purity was confirmed by NMR measurements and elemental analysis. ³¹P NMR shows only a single peak at 7.389 ppm. ¹H NMR: 2.996 ppm (–CH₃, s, 6H), 3.374 ppm (N–CH₂–P, d, 4H, J_{H-P} = 12.6 Hz), 3.736 ppm (N–CH₂–C, s, 4H). Elemental analysis for $C_6H_{18}N_2O_6P_2$: C, 25.91; H, 6.32; N, 10.25; P, 22.38. Calc. C, 26.07; H, 6.52; N, 10.14; P, 22.45%. The single crystals of **1** were obtained from the aqueous solution of the diphosphonic acid and cobalt(II) nitrate in a molar ratio of 1:1. The cobalt(II) diphosphonate was not formed due to the high acidity of the solution. In a similar reaction[4b] between $Co(ClO_4)_2$ and an azacrownphosphonic acid, a proton was transferred from the solution to the phosphonic acid producing a hydrogen-bonded linear chain free of Co^{2+}.

Synthesis of Ni(H₂L)(H₂O)₂ 2. $NiCl_2 \cdot 6H_2O$ (1 mmol, Fisher), *N,N*'-dimethyl-*N,N*'-ethylenediamine-bis(methylenephosphonic acid) (H₄L, 1 mmol) and tetraethylammonium chloride (5 mmol, Kodak) were mixed and dissolved into 10.0 ml of deionized water, then the pH value of the resultant solution was adjusted to approximately 6 by adding 40 wt.% tetrabutylammonium hydroxide solution (Aldrich). Green crystals of **2** were recovered in 35.7% yield after two weeks. Elemental analysis for **2**, $C_6H_{20}N_2O_8P_2Ni$: C, 19.32; H, 5.37; N, 7.68; P, 16.85. Calc. C, 19.54; H, 5.46; N, 7.59; P, 16.79%.

Synthesis of Pb(H₂L) 3. Complex **3** was synthesized by hydrothermal reactions. A mixture of 1.0 mmol of lead acetate trihydrate (Aldrich), 1.0 mmol of *N,N*'-dimethyl-*N,N*'-ethylenediamine-bis(methylenephosphonic acid) (H₄L) and 10.0 ml of deionized water was sealed into a bomb equipped with a Teflon liner, and then heated at 150 °C for 4 days. Colorless crystals of **3** were recovered in *ca.* 77.5% yield (0.373 g). Results of the ³¹P solid state MAS NMR measurements showed a single peak at 22.8 ppm. Elemental analysis for **3**, $C_6H_{16}N_2O_6P_2Pb$: C, 14.82; H, 3.46; N, 5.97; P, 12.73. Calc. C, 14.97; H, 3.35; N, 5.82; P, 12.87%.

Crystallography

Single crystals of H₄L **1**, Ni(H₂L)(H₂O)₂ **2** and Pb(H₂L) **3** were mounted on a Bruker Smart CCD using MoKα radiation (λ = 0.71069 Å), and a graphite monochromator at temperatures of 110(2), 110(2) and 100(2) K, respectively. The cell constants were indexed from reflections obtained from 60 frames collected with 10 seconds exposure per frame. A hemisphere of data (1271 frames at 5 cm detector distances) was collected by the narrow-frame method with scan widths of 0.30° in ω and exposure time of 20, 20 and 30 seconds per frame for **1**, **2** and **3**, respectively. The first 50 frames were recollected in the end of data collection to assess the stability of the crystal, and

it was found that the decay in intensity was less than 1%. The data were corrected for the Lorentz factor, polarization, air absorption and absorption due to variations in the path length through the detector faceplate. Absorption corrections based on the ψ scan method were also applied to all three data sets.[14]

The space groups were determined from systematic absences to be $P2_1/n$ (No. 14), $P2/n$ (No. 13) and $C2/m$ (No. 12) or their corresponding non-centrosymmetric groups for **1**, **2** and **3**, respectively. The structures were solved using direct methods (SHELXTL) and refined by least-square methods with atomic coordinates and anisotropic thermal parameters for all non-hydrogen atoms in the centric space groups.[14] All hydrogen atoms were generated geometrically, assigned fixed isotropic thermal parameters and included in the structure factor calculations. The highest residual peaks are 0.498 e Å³ (for **1**), 1.777 e Å³ (for **2**, 0.78 Å from Ni1 atom) and 2.865 e Å³ (for **3**, 0.93 Å from Pb1 atom), respectively. Satisfactory refinement in the centrosymmetric space groups indicated their correctness. Some of the data collection and refinement parameters are summarized in Table 1. Important bond lengths and angles for **1**, **2** and **3** are listed in Table 2.

CCDC reference numbers 195094–195096.

See http://www.rsc.org/suppdata/dt/b2/b206343n/ for crystallographic data in CIF or other electronic format.

Results and discussion

The asymmetric unit of **1** is shown in Fig. 1. The diphosphonic
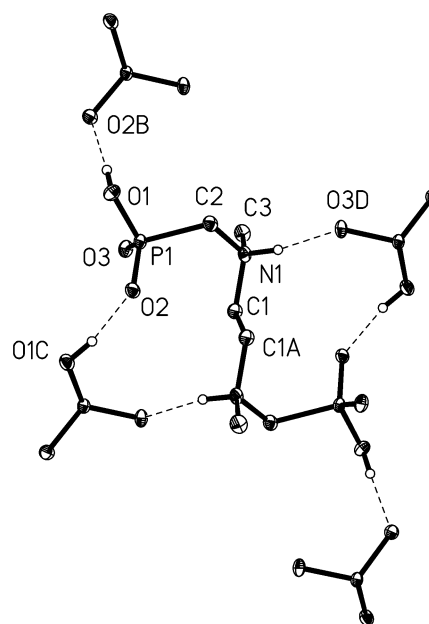

Fig. 1 ORTEP representation of the asymmetric unit of **1**. Thermal ellipsoids are drawn at 50% probability. The dashed lines represent hydrogen bonds.

acid is located on a center of symmetry, as shown in Fig. 1. It occurs in a zwitterionic form, *i.e.* each phosphonic group transfers one proton to an amine group. The P1–O1 distance is significantly larger than the remaining two P–O distances, thus O1 is the most likely to be protonated. Both phosphonate oxygen atoms and amine nitrogen atoms are involved in hydrogen bonding with the O1–H ··· O2 distance being extremely short. Neighboring molecular units are interconnected by hydrogen bonds into a <10$\bar{1}$> 2D layer (Fig. 2). Along the *b*-axis, the molecular units are interconnected by N1–H11a ··· O3 hydrogen bonds, whereas they are interlinked by O1–H1a ··· O2 hydrogen bonds along the diagonal direction of the *a*- and *c*-axes. Neighboring 2D layers are held together by van der Waals forces (Fig. 3).

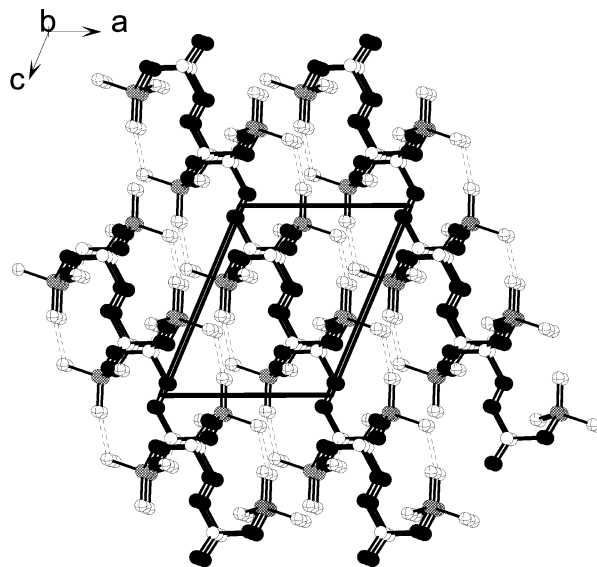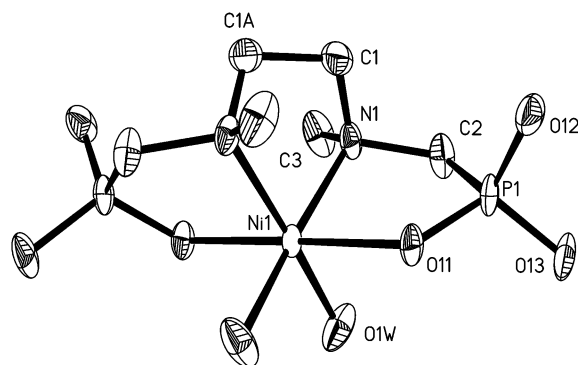**Table 1** Crystal data and structure refinement for **1**, **2** and **3**

Compound	**1**	**2**	**3**
Formula	$C_6H_{18}N_2O_6P_2$	$C_6H_{20}N_2O_8P_2Ni$	$C_6H_{16}N_2O_6P_2Pb$
M	276.16	368.89	481.34
Crystal system	Monoclinic	Monoclinic	Monoclinic
Space group	$P2_1/n$ (No. 14)	$P2/n$ (No. 13)	$C2/m$ (No. 12)
$a/\text{Å}$	6.9401(15)	8.302(7)	17.202(3)
$b/\text{Å}$	10.456(2)	9.042(7)	8.8751(14)
$c/\text{Å}$	8.4868(18)	9.932(8)	8.2710(13)
$\beta/°$	112.844(4)	105.014(3)	112.577(13)
$V/\text{Å}^3$	567.5(2)	688.4(9)	1219.7(3)
Z	2	2	4
μ/mm^{-1}	0.400	1.677	14.113
Reflections collected	3330	4068	3670
Independent reflections	1279 (R_{int} = 0.0402)	1571 (R_{int} = 0.0475)	1384 (R_{int} = 0.1056)
$R1/wR2$ ($I > 2\sigma(I)$ data)	0.0373/0.1069	0.0613/0.1655	0.0391/0.0770
$R1/wR2$ (all data)	0.0425/0.1154	0.0705/0.1692	0.0461/0.0785

$R1 = \Sigma||F_o| - |F_c||/\Sigma|F_o|$, $wR2 = \{\Sigma w[(F_o)^2 - (F_c)^2]^2/\Sigma w[(F_o)^2]^2\}^{1/2}$.
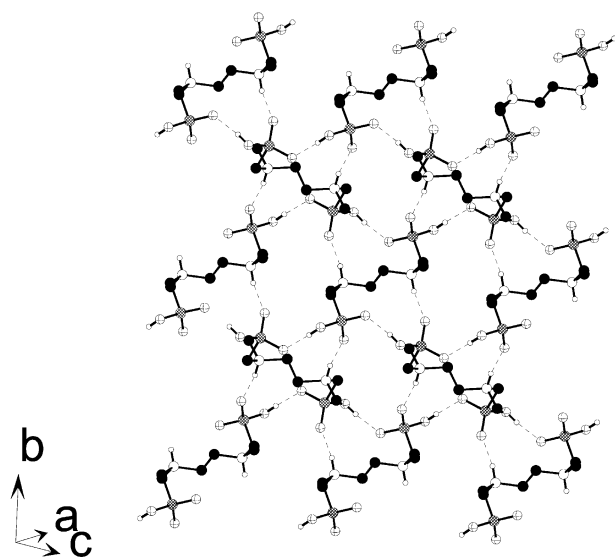
Fig. 2 A <10$\bar{1}$> layer of **1**. P, C, O, H and N atoms are represented as hatched, black, crossed small open and large open circles, respectively. The dotted lines represent hydrogen bonds.

Fig. 3 View of structure of **1** down the *b*-axis.

The Ni(II) ion in **2** is octahedrally coordinated by a chelating ligand (2N1 and 2O11) and two aqua ligands (Fig. 4). The Ni–N, Ni–O(phosphonate) and Ni–O(water) distances are 2.121(4), 2.074(4) and 2.052(4) Å, respectively. These Ni(H$_2$L)(H$_2$O)$_2$ units are further interlinked by hydrogen bonds between uncoordinated phosphonate oxygen atoms, resulting a <020> hydrogen bonded double layer (Fig. 5). The nearest Ni(II) · · · Ni(II) distance is 5.647(1) Å. The hydrogen bond distances are 2.495 Å (O12 · · · O12) and 2.480 Å (O13 · · · O13). Such hydrogen-bonded double layers are packed *via* van der Waals forces along the *b*-axis (Fig. 5). The interlayer distance corresponds to the length of the *b*-axis (9.042(7) Å). The two nitrogen atoms are deprotonated which allow them to coordinate to the metal ion. This differs greatly from the behavior of the nitrogen atom in the metal complexes with phosphonic acids that contain only one nitrogen atom. Such nitrogen atoms are normally protonated and not coordinated to the metal ions.[9,10]

The phosphonate groups are 1H-protonated, as in the free ligand, however, it is not easy to locate the proton since the P1–O12 and P1–O13 distances are very close. Based on the O12 · · · O12 and O13 · · · O13 distances, we think the proton is disordered over 2 sites, switching between O12 and O13, aided by the close approach of the oxygens.

Fig. 4 ORTEP representation of the asymmetric unit of **2**. Thermal ellipsoids are drawn at 50% probability.

As shown in Fig. 6, the lead(II) ion in **3** is 6-coordinated by two nitrogen atoms and two phosphonate oxygen atoms of a single ligand and two phosphonate oxygen atoms from two neighboring Pb(H$_2$L) units. The coordination geometry around the lead(II) ion can be described as a distorted octahedron. The Pb–O and Pb–N distances are 2.478(4) and 2.564(4) Å, respectively. Each ligand chelates with a Pb(II) ion tetradentately (2N1 and 2O11), the μ^2 O11 atom is also coordinated to a lead(II) ion from the neighboring Pb(H$_2$L) unit; this type of coordination

Table 2 Bond lengths [Å] and angles [°] for **1**, **2** and **3**

1

P(1)–O(3)	1.5033(15)	P(1)–O(2)	1.5081(15)
P(1)–O(1)	1.5541(16)	P(1)–C(2)	1.834(2)
N(1)–C(3)	1.494(2)	N(1)–C(1)	1.500(3)
N(1)–C(2)	1.500(3)	C(1)–C(1)#1	1.521(4)

Hydrogen bonds

O(1) · · · O(2)#2	2.475	O(1)–H(1A) · · · O(2)#2	165.7
N(1) · · · O(3)#3	2.641	N(1)–H(11A) · · · O(3)#3	169.1

O(3)–P(1)–O(2)	115.98(9)	O(3)–P(1)–O(1)	113.62(9)
O(2)–P(1)–O(1)	108.11(8)	O(3)–P(1)–C(2)	108.99(9)
O(2)–P(1)–C(2)	106.66(9)	O(1)–P(1)–C(2)	102.40(9)
C(3)–N(1)–C(1)	109.73(16)	C(3)–N(1)–C(2)	111.82(16)
C(1)–N(1)–C(2)	115.01(16)	N(1)–C(1)–C(1)#1	110.1(2)
N(1)–C(2)–P(1)	116.02(13)		

2

Ni(1)–O(1W)#1	2.052(4)	Ni(1)–O(1W)	2.052(4)
Ni(1)–O(11)	2.074(4)	Ni(1)–O(11)#1	2.074(4)
Ni(1)–N(1)	2.121(4)	Ni(1)–N(1)#1	2.121(4)
P(1)–O(11)	1.510(4)	P(1)–O(12)	1.528(4)
P(1)–O(13)	1.535(4)	Ni(1) · · · Ni(1)#3	5.647(1)

Hydrogen bonds

O(12) · · · O(12)#2	2.495	O(13) · · · O(13)#3	2.480

O(1W)#1–Ni(1)–O(1W)	91.4(3)	O(1W)#1–Ni(1)–O(11)	88.76(14)
O(1W)–Ni(1)–O(11)	90.36(14)	O(1W)#1–Ni(1)–O(11)#1	90.36(14)
O(1W)–Ni(1)–O(11)#1	88.76(14)	O(11)–Ni(1)–O(11)#1	178.7(2)
O(1W)#1–Ni(1)–N(1)	171.69(15)	O(1W)–Ni(1)–N(1)	92.9(2)
O(11)–Ni(1)–N(1)	84.08(14)	O(11)#1–Ni(1)–N(1)	96.86(15)
O(1W)#1–Ni(1)–N(1)#1	92.9(2)	O(1W)–Ni(1)–N(1)#1	171.69(15)
O(11)–Ni(1)–N(1)#1	96.86(15)	O(11)#1–Ni(1)–N(1)#1	84.08(14)
N(1)–Ni(1)–N(1)#1	83.8(3)		

3

Pb(1)–O(11)#1	2.478(4)	Pb(1)–O(11)	2.478(4)
Pb(1)–N(1)#1	2.564(4)	Pb(1)–N(1)	2.564(4)
Pb(1)–O(11)#2	2.634(4)	Pb(1)–O(11)#3	2.634(4)
P(1)–O(12)	1.518(4)	P(1)–O(11)	1.522(4)
P(1)–O(13)	1.549(4)	Pb(1) · · · Pb(1)#3	4.157(1)

Hydrogen bonds

O(13) · · · O(12)#4	2.503	O(13)–H(13A) · · · O(12)#4	166.0

O(11)#1–Pb(1)–O(11)	160.0(2)	O(11)#1–Pb(1)–N(1)#1	71.40(14)
O(11)–Pb(1)–N(1)#1	92.16(14)	O(11)#1–Pb(1)–N(1)	92.16(14)
O(11)–Pb(1)–N(1)	71.40(14)	N(1)#1–Pb(1)–N(1)	72.0(2)
O(11)#1–Pb(1)–O(11)#2	71.23(14)	O(11)–Pb(1)–O(11)#2	115.71(16)
N(1)#1–Pb(1)–O(11)#2	132.47(14)	N(1)–Pb(1)–O(11)#2	81.14(14)
O(11)#1–Pb(1)–O(11)#3	115.71(16)	O(11)–Pb(1)–O(11)#3	71.23(14)
N(1)#1–Pb(1)–O(11)#3	81.14(14)	N(1)–Pb(1)–O(11)#3	132.47(14)
O(11)#2–Pb(1)–O(11)#3	142.4(2)		

Symmetry transformations used to generate equivalent atoms: For **1**: #1 −x + 1, −y + 1, −z + 1 #2 x − 1/2, −y + 1/2, z − 1/2 #3 −x + 1/2, y + 1/2, −z + 1/2. For **2**: #1 −x + 1/2, y, −z − 1/2 #2 −x + 1/2, y, −z + 1/2 #3 −x, −y + 1, −z. For **3**: #1 −x + 1, y, −z + 3/2 #2 x, −y + 1, z − 1/2 #3 −x + 1, −y + 1, −z + 2 #4 −x + 1/2, −y + 3/2, −z + 2.

mode is different from that in **2** (Fig. 4). Each phosphonate group of the ligand in **3** is 1H-protonated, which is similar to that of the free ligand molecule discussed above (Fig. 1) and that in **2**. From the P–O distances, the O13 atom is most likely to be protonated (see Table 2). Both O12 and O13 atoms are not coordinated to the metal ion, but form strong hydrogen bonds, the O(13) · · · O(12) distance is 2.503 Å and the hydrogen bond angle (O13–H13A · · · O12) is 166.0°. These hydrogen bonds are slightly weaker than those in **1** and **2**. Two Pb(H$_2$L) units are interconnected through a pair of bridging phosphonate oxygen atoms, resulting in one dimensional chains along the c-axis direction (Fig. 7), the distance between two neighboring Pb(II) ions is 4.157(1) Å, which is much shorter than that of the Ni · · · Ni distance in **2**. Such chains are held together *via* hydrogen bonds between uncoordinated phosphonate oxygen

atoms into a <1$\bar{1}$0> layer (Fig. 7), and such layers are further interlinked through hydrogen bonds, resulting in a 3D network (Fig. 8).

2 began to lose two coordination water molecules at 150 °C, the weight loss of 9.20% is in good agreement with the calculated value (9.87%). Then it continued to lose weight up to 1000 °C; this involves two steps that are overlapped, first, the release of one water molecule formed by the condensation of two hydrogen phosphonate groups and second, the burning of the organic group. The final product is Ni(PO$_3$)$_2$, the total weight loss is 40.6%, which matches the theoretical value quite well (40.6%). The TGA diagram for **3** indicates that the complex is stable up to 306°. Then it shows a one step weight loss that is completed at about 750°, during this process, two reactions occurred simultaneously: first, the release of one water
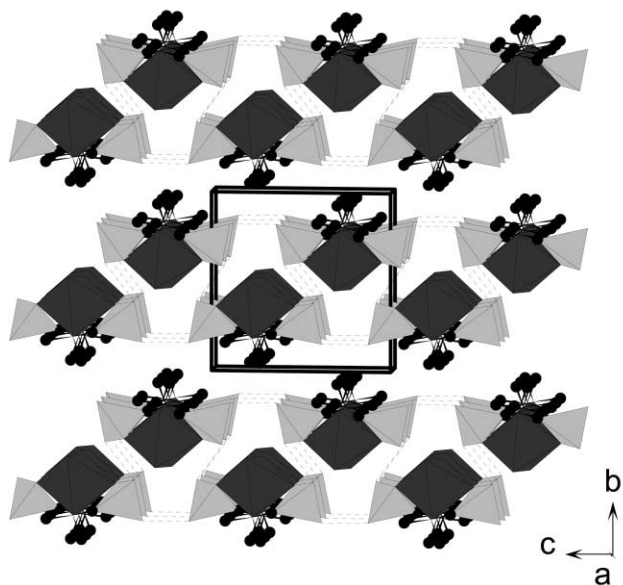
Fig. 5 Packing of the hydrogen bonded <020> double layer of **2** along the *b*-axis. NiN$_2$O$_4$ octahedra and C–PO$_3$ tetrahedra are shaded in dark and light gray, respectively. Carbon atoms are drawn as black circles.
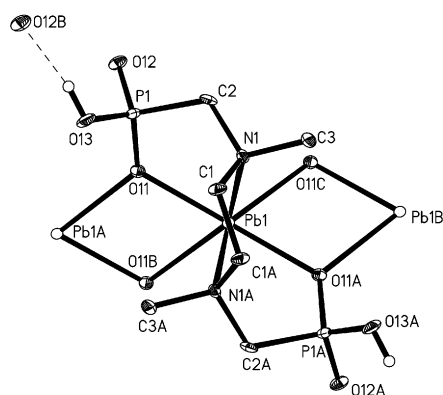

Fig. 6 ORTEP representation of the asymmetric unit of **3**. Thermal ellipsoids are drawn at 50% probability. The dotted lines indicate hydrogen bonds.
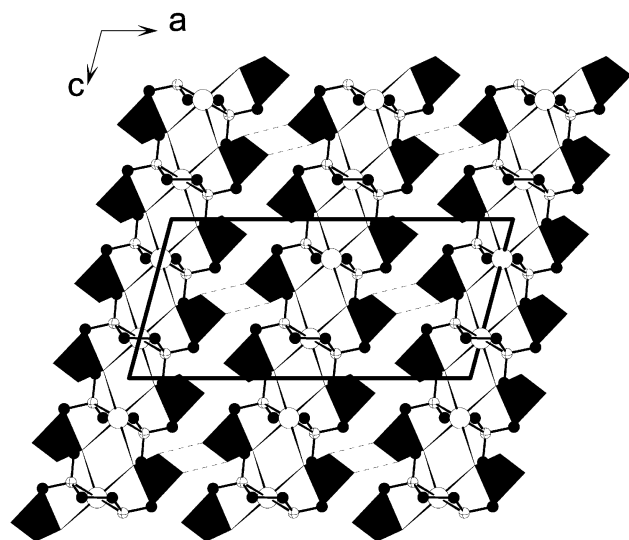

Fig. 7 Polyhedral representation of a hydrogen-bonded <1$\bar{1}$0> layer of **3**. C–PO$_3$ tetrahedra are shaded in black. Pb, N and C atoms are shown as large open, crossed and black circles, respectively. The dashed lines indicate hydrogen bonds.

molecule formed by the condensation of two hydrogen phosphonate groups and second, the burning of the organic group. The total weight loss is 25.0%, which is in good agreement with
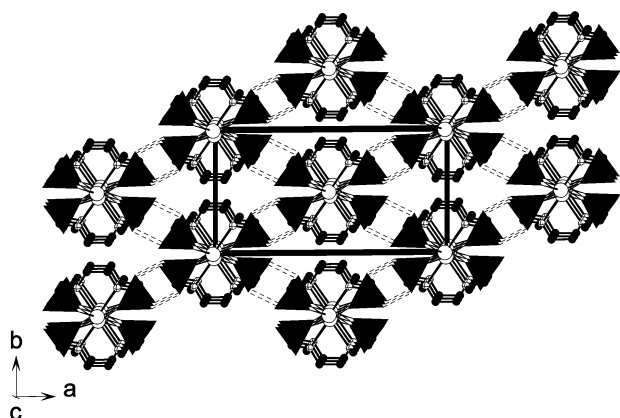

Fig. 8 View of crystal structure of **3** along *c* the axis, which together with the view in Fig. 7 illustrates the 3D nature of the hydrogen bonding.

the calculated weight loss of 24.14% if the final products are assumed to be lead metaphosphate [Pb(PO$_3$)$_2$].

Plot of the $\chi_M T$ *versus* T (χ_M being the magnetic susceptibility per mole of the metal atoms) for **2** is shown in Fig. 9. At
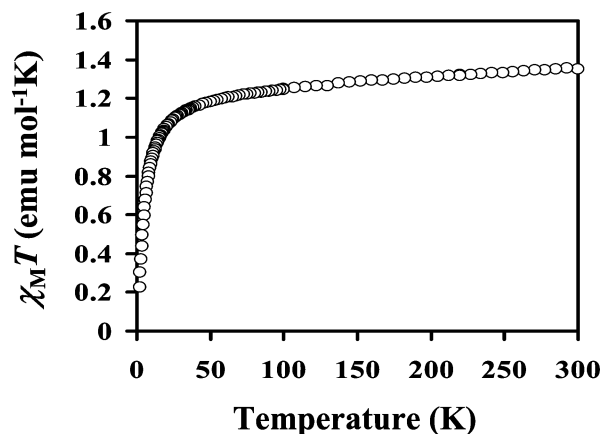

Fig. 9 Plot of $\chi_M T$ *versus* T for **2**.

room temperature the measured $\chi_M T$ of 1.35 emu mol^{-1} K, which corresponds to an isolated nickel(II) ion with $S = 1$ (1.26 emu mol^{-1} K).[15] At 2 K, the $\chi_M T$ value is decreased to 0.23 emu mol^{-1} K. The measured Curie constant is 1.365 emu-K mol^{-1}, which is slightly larger than the calculated value (1.21 emu-K mol^{-1}). μ_{eff} calculated from the value of C is 3.30, somewhat higher than the 2.83 μ_β expected for two unpaired electrons based on the spin only formula. The θ value is calculated to be -7.094 K, thus there is significant antiferromagnetic interaction between two Ni(II) ions from two neighboring Ni(H$_2$L) units (Ni $\cdots$ Ni 5.647(1) Å).

Conclusions

Replacement of two protons of the diphosphonic acid (H$_4$L) **1** by divalent Ni(II) and Pb(II) ions resulted in two new metal(II) phosphonates, Ni(H$_2$L)(H$_2$O) **2** and Pb(H$_2$L) **3**. The phosphonate groups in all three compounds are 1H-protonated, thus are capable of hydrogen bond formation. These hydrogen bonds connect the molecular units of **1** and **2** into a hydrogen bonded layer or double layer; such a layer of **3** is built from 1D Pb(H$_2$L) chains. The ligand molecule in both **2** and **3** adopts a tetradentate chelating coordination mode to form a M(H$_2$L) unit. The octahedral coordination geometry of the Ni(II) ion is satisfied by two aqua ligands in **2**, whereas that of the Pb(II) ion is saturated by two μ^2 bridging phosphonate oxygen atoms from neighboring M(H$_2$L) units, resulting in a 1D metal phos-

phonate chain. Further studies will be aimed at the synthesis of its 2D metal phosphonates, which may be achieved by further deprotonation of the diphosphonic acid, or reactions at lower pH values where the nitrogen atoms remain protonated.

Acknowledgements

References

1 (*a*) E. W. Stein Sr., A. Clearfield and M. A. Subramanian, *Solid State Ionics*, 1996, **83**, 113; (*b*) G. Alberti and U. Costantino, in *Comprehensive Supramolecular Chemistry*, ed. J. M. Lehn, Pergamon-Elsevier Science Ltd., London, 1996, p. 1; (*c*) A. Clearfield, *Curr. Opin. Solid State Mater. Sci.*, 1996, **1**, 268; (*d*) A. Clearfield, *Metal phosphonate chemistry* in *Progress in Inorganic Chemistry*, ed. K. D. Karlin, John Wiley & Sons, New York, 1998, vol. 47, pp. 371–510 and references therein.

2 M. E. Thompson, *Chem. Mater.*, 1994, **6**, 1168.

3 G. Alberti and U. Costantino, in *Comprehensive Supramolecular Chemistry*, ed. J. M. Lehn, Pergamon-Elsevier Science Ltd., London, 1996, p. 151.

4 (*a*) B. Zhang and A. Clearfield, *J. Am. Chem. Soc.*, 1997, **119**, 2751; (*b*) C. V. K. Sharma and A. Clearfield, *J. Am. Chem. Soc.*, 2000, **122**, 1558; (*c*) I. Lukes, J. Kotek, P. Vojtisek and P. Hermann, *Coord. Chem. Rev.*, 2001, **216–217**, 287; (*d*) A. Clearfield, D. M. Poojary, B. Zhang, B. Zhao and A. Derecskei-Kovacs, *Chem. Mater.*, 2000, **12**, 2745; (*e*) J.-G. Mao, Z. Wang and A. Clearfield, *Inorg. Chem.*, 2002, **41**, 3713.

5 (*a*) B. Zhang, D. M. Poojary, A. Clearfield and G.-Z. Peng, *Chem. Mater.*, 1996, **8**, 1333; (*b*) D. M. Poojary and A. Clearfield, *J. Organomet. Chem.*, 1996, **512**, 237; (*c*) D. M. Poojary, B. Zhang and A. Clearfield, *Angew. Chem., Int. Ed.*, 1994, **33**, 2324.

6 B. Zhang, D. M. Poojary and A. Clearfield, *Inorg. Chem.*, 1998, **37**, 249.

7 J.-G. Mao and A. Clearfield, *Inorg. Chem.*, 2002, **41**, 2319.

8 S. O. H. Gutschke, D. J. Price, A. K. Powell and P. T. Wood, *Angew. Chem., Int. Ed.*, 1999, **38**, 1088.

9 (*a*) J.-G. Mao, Z. Wang and A. Clearfield, *Inorg. Chem.*, 2002, **41**, 2334; (*b*) J.-G. Mao, Z. Wang and A. Clearfield, *New J. Chem.*, 2002, **26**, 1010.

10 (*a*) C. V. K. Sharma, A. Clearfield, A. Cabeza, M. A. G. Aranda and S. Bruque, *J. Am. Chem. Soc.*, 2001, **123**, 2885; (*b*) A. Cabeza, X. Ouyang, C. V. K. Sharma, M. A. G. Aranda, S. Bruque and A. Clearfield, *Inorg. Chem.*, 2002, **41**, 2325.

11 (*a*) M. Yu. Antipin, A. P. Baranov, M. I. Kabachnik, T. Ya. Medved', Yu. M. Polikarpov, Yu. T. Struchkov and B. K. Shcherbakov, *Dokl. Akad. Nauk SSSR*, 1986, **287**, 130; (*b*) M. I. Kabachnik, M. Yu. Antipin, B. K. Shcherbakov, A. P. Baranov, Yu. T. Struchkov, T. Ya. Medved' and Yu. M. Polikarpov, *Koord. Khim.*, 1988, **14**, 536; (*c*) S. W. A. Bligh, N. Choi, C. F. G. C. Geraldes, S. Knoke, M. McPartlin, M. J. Sanganee and T. M. Woodroffe, *J. Chem. Soc., Dalton Trans.*, 1997, 4119.

12 (*a*) I. Lukes, J. Kotek, P. Vojtisek and P. Hermann, *Coord. Chem. Rev.*, 2001, **216–217**, 287; (*b*) J. Kotek, P. Hermann, I. Císařová, J. Rohovec and I. Lukeš, *Inorg. Chim. Acta*, 2001, **317**, 324.

13 (*a*) L. M. Shkol'nikova, A. L. Poznyak, V. K. Bel'skii, M. V. Rudomino and N. M. Dyatlova, *Koord Khim.*, 1986, **12**, 981; (*b*) L. M. Shkol'nikova, M. A. Porai-Koshits, V. S. Fundamenskii, A. L. Poznyak and E. V. Kalugina, *Koord Khim.*, 1991, **17**, 954.

14 G. M. Sheldrick, SHELXTL, Crystallographic Software Package, version 5.1, Bruker-AXS, Madison, WI, 1998.

15 B. Zurowska, J. Mroziński, M. Julve, F. Lloret, A. Maslejova and W. Sawka-Dobrowolska, *Inorg. Chem.*, 2002, **41**, 1771.